International Journal of Trend in Scientific Research and Development (IJTSRD)
Volume 5 Issue 4, May-June 2021 Available Online: www.ijtsrd.com e-ISSN: 2456 – 6470

The Graphene Based Materials Used in Energy

Tarun Radadiya

Researcher & PG Data Science Student of Amity University, Noida, Uttar Pradesh, India

ABSTRACT

Graphene two-dimensional carbon sheet with one atom thickness and one of the thinnest materials in universe. However, pure Graphene sheets are limited for many applications despite their excellent characteristics and scientists face challenges to induce more and controlled functionality. The nanomaterials inherit the unique properties of Graphene, and the addition of functional groups or the nanoparticle composites on their surfaces improves their performance. Therefore Graphene nanocomposites or hybrids are attracting increasing efforts for real applications in energy and environmental areas by introducing controlled functional building blocks to Graphene. Nanocomposites energy-related progress of Graphene nanocomposites in solar energy conversion (e.g., photovoltaic and photo electrochemical devices, artificial photosynthesis) and electrochemical energy devices (e.g., lithium ion battery, super capacitor, fuel cell). The Graphene nanocomposites advances in environmental applications of functionalized Graphene nanocomposites for the detection and removal of heavy metal ions, organic pollutants, gas and bacteria, treatment of environmental pollution, environmental protection and detection. Graphene nanocomposites in energy and environmental science.

KEYWORDS: *Graphene, pure Graphene sheet, Graphene nanocomposites, environment application, energy application*

How to cite this paper: Tarun Radadiya "The Graphene Based Materials Used in Energy" Published in International Journal of Trend in Scientific Research and Development (ijtsrd), ISSN: 2456-6470, Volume-5 | Issue-4, June 2021, pp.1140-1147, URL: www.ijtsrd.com/papers/ijtsrd42512.pdf

IJTSRD42512

INTRODUCTION:

Graphene itself has weak absorption for light, making pure graphene sheets not suitable for collecting solar light efficiently. The capacitance of graphene is limited by the electronic double-layer regime and is very low. Therefore large-scale practical applications of graphene face the challenge to induce more and controlled functionality to pure graphene sheets.

Although graphene sheets were mostly explored in fundamental physics at the beginning, graphene nanocomposites or hybrids are attracting increasing efforts for real applications

[1-8]. The recent focus on graphene as a general platform for nanocomposites has inspired many possibilities in energy and environmental aspects by introducing controlled functional building blocks to graphene [9-18]. Many methods have been developed to prepare functionalized graphene nanocomposites. Covalent and noncovalent methods, chemical electroless deposition, hydrothermal and solvothermal growth, electrochemical and electrophoresis deposition, photochemical reaction, and physical deposition and mixing are intensively pursued to prepare well-defined functional graphene nanocomposites.

To introduce controlled functionality to graphene, molecules, nanoscale objects and polymers are applied to functionalize graphene toward specific applications[14-15]. Various functional graphene nanocomposites have demonstrated strong potential in energy devices and have been applied for solar energy conversion (such as photovoltaic and photoelectrochemical cells and artificial photosynthesis), and electrochemical energy devices (lithium ions battery, supercapacitor, fuel cell). In addition to energy applications, functionalized graphene nanocomposites are also excellent platforms for environmental applications in the detection and removal of heavy metal ions, organic pollutants, gas and bacteria.

Graphene has a surface area of 2630 $m^2 g^{-1}$, a mobility of 200 000 $cm^2 V^{-1} s^{-1}$ at a carrier density of ~1012 cm^{-2}, and the highest electrical conductivity at room temperature (10^6 s cm^{-1})[19-21]. The strong mechanical properties of graphene with a Young's modulus of ~1 TPa and breaking strength of 42 N m^{-1} and excellent thermal conductivity (~5000 W m^{-1} K^{-1}) are also favorable for various graphene applicatons [22,23]. Graphene absorbs 2.3% light over a broad wavelength range for each layer which makes graphene transparent and suitable for specific optoelectronic applications [24]. The fast development in the graphene field has suggested the great potential of graphene in electronics, optoelectronics, and electrochemical and biomedical applications due to its unique structure and properties [25-34].

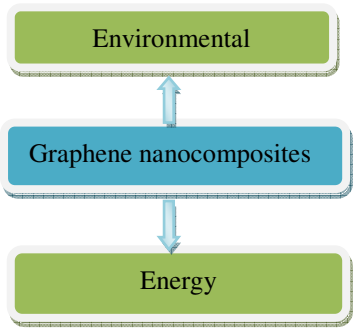

Figure:-1 Graphene nanocomposites application

The progress made in graphene-based nanocomposites has been scattered in several reviews either with a focus on specific materials such as inorganic materials or polymers, or on specific applications in energy[5,7-14,17,18] However, a whole view of graphene nanocomposites from general preparation methods and functionalizations with all kinds of materials However, pure graphene sheets are limited for many applications despite (molecules, nanoscale objects and polymers) to both energy and environmental applications is still missing. But progress made in graphene nanocomposites preparation methods, functionalization methods, and in their applications in energy and environmental areas. The preparation and functionalization methods of graphene nanocomposites are firstly introduced followed by recent progress in energy and environmental studies.

Graphene energy application

Solar cell

As a two-dimensional (2D)giant flat molecule, graphene possesses a few outstanding electrical and optical properties, such as extremely high carrier mobility[35], micro-scale ballistic transport[36],abnormal quantum Hall effect[37], 2.3% constant absorption of visible light[38].Besides, it slow density of energy states near Dirac point and tunable doping concentration discriminate graphene from thin metalsand traditional semiconductors[39]. Graphene also has extraordinary thermal conductivity [40] and high mechanical strength[41]. All these as pects make graphene a well-defined 'alien'in human-developed materials [35,42]. Attracted by those fascinating properties, graphene/semiconductor hetero structures are promising for solar cells applications [43-48]. Among them, graphene/silicon(Si) solar cell is most popularand much attention has been dedicated toit[49-53]. The state of art Eta of graphene/Sisolar cell is limited to 8.6% [54] and 14.5%[49], without and with anti-reflection coating (ARC), respectively. Compared with Si, GaAs is commonly used to fabricate high efficient solar cells[55-58].Suitable direct band gapenergy of 1.42eV and high electron mobility (8000cm^2/V·s at 300K[59]), which is about six times of that of Si (1350 cm^2/V·s at 300K[60]), make GaA sone of the best candidates for high performance solar cells[61].Until now, there is rare work ongraphene/GaAs solar cells[62]. Jieet al reported graphene/GaAs solar cellswhich can only convert 1.95% of input light into electricity [63], which is poor considering the advantages of GaAs over Si. Thus, a deep insight into graphene/GaAs solar cellsis highly needed. Herein, we have achieved high performance solar cells with Eta of 10.4%for doped graphene/GaAs structure. Through anti-reflection technique, Etahas been further improved up to 15.5%, which is higher than the state of art Etafor graphene/Si system. It is noteworthy that 25.8% of Eta can be reasonably calculated for the van der Waals Schottky diode formed between graphene and GaAs, promising the practical application of graphene/GaAs hetero structure in solar cells.

Structure of the graphene/GaAs solar cells

The schematic structure of the graphene/GaAs solar cell is illustratedin Figure 2, which is composed of GaAs substrate, graphene and electrodes. A SiNx film is sandwiched between graphene and GaAs as the dielectric insulating layer. The GaAs substrate is heavily n-type doped, which has a resistivity of 0.01-0.1 Ωcm. Nearly 50 graphene/GaAs solar cells have been fabricated in this work while the digital photograph of the typical graphene/GaAs solar cells. The Raman spectrum of graphene is shown in Figure 3, where very weak defect-related D peak (around 1350 cm^{-1}) indicates the high quality of graphene. As seen from Figure 3, the G peak of as-grown graphene is located around 1596 cm^{-1}, which is blue-shifted compared with1580$cm^{-1}$of undoped graphene, indicating as-grown graphene is p-type doped.

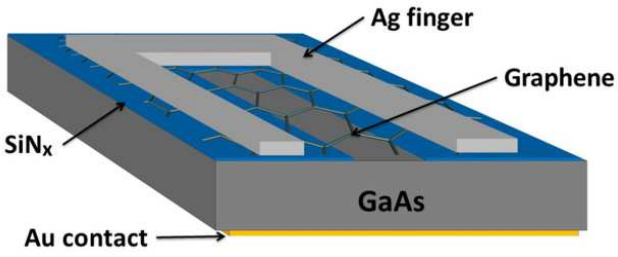

Figure:-2 Graphene/GaAssolar cells.Schematic structure of the graphene/GaAssolar cell.

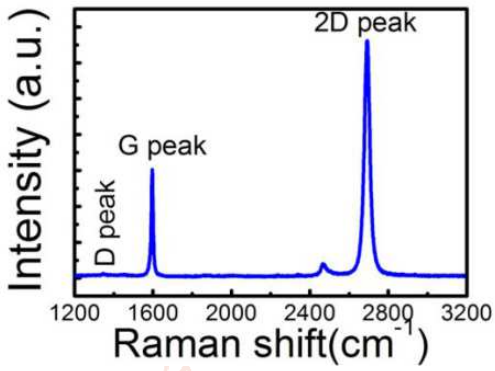

Figure:-3 Raman spectrum of monolayer graphene in the devices.

Depending of solar cell performance on graphene layer numbers

The schematic electronic band structure of graphene/GaAs Schottky diode is displayed in Figure 4a. As the GaAs substrate is heavily n-type doped, its work function (Φn-GaAs in Figure 4a) is in the range of 4.07±0.05eV, close to its electron affinity (4.07 eV)[64]. The electron affinity, i.e. energy difference between vaccum level and Dirac point of graphene is about 4.6eV[65]. As the Fermi level of graphene can be well adjusted by doping, its work function (Φgraphene in Figure 4a) is varied according to the doping concentration. When GaAs touches with graphene by van der Waals forces, Schottky junction is formed with a build-in barrier and a depletion region in GaAs. As the screening length of grapheneis less than0.5 nm[66]and GaAs is in bulk form, the traditional analysis based on bulk semiconductor physicsis granted for graphene/GaAs heterostructure. The barrier height of this Schottky junction (Φbarrier in Figure 4a) is the difference between Φn-GaAs and Φgraphene. Dark current density-voltage (J-V) curve of the graphene/GaAs Schottky junction can be expressed by equation1:

$$J=Jo = (\exp \frac{qV}{NIFKT} - 1)$$

Where K is the Boltzmann constant, NIF is the junction ideality factor; q is the value of electron charge. Based on thermionic-emission theory, Jo can be described as:

$$Jo=AT^2 \exp (- \frac{q\Phi \text{ barrier}}{KT})$$

where A is the effective Richardson's constant of GaAs ($8.9A/k{\cdot}cm^2$) [67], Φbarrier is the biuld-in junction barrier height. Under light illumination, the electrons and holes produced in GaAs substrate will be seperated by this Schottky junction and transport through GaAs and graphene, respectively

The Eta of the Schottky junction depends on the short circuit current density (Jsc), open circuit voltage (Voc) and fill factor (FF) based on the following equation: Eta=Voc×Jsc×FF. Several papers have reported that graphene layer numbers affects the performance of this type solar cells [71,68,69]. In order to optimize graphene/GaAs solar cell, devices with different layer numbers of graphene are studied. The experimental value of Voc for the devices using as-grown graphene shows monotonically decreasing trend as the layer number increases, as shown in Figure 4b. Voc of the graphene/GaAs Schottky diode is affected by carrier lifetime in bulk (τbulk)and surface(τsurface), Φbarrier and NIF, which are independent in traditional solar cells[70].It can be expected that increasing the layer numbers of graphene will decrease Jsc, which is induced by the enhanced light absorption of graphene layers. Monolayer graphene absorbs 2.3% of sun light[72], which is assumed to be dissipated and cannot be converted into electricity. Thus, Jsc of the solar cells with multi-layers graphene is calculated through subtracting 2.3% from the experimental value of monolayer graphene/GaAs device while adding one more layer of graphene on the device. However, it is reason able assumed that some of holes produced in GaAs are eliminated by defects or impurities while hopping among graphene layers. Thus, interlayer recombination is enhanced and τsurface is reduced while stacking multilayer graphene over GaAs. Indeed, as shown in Figure 4c,

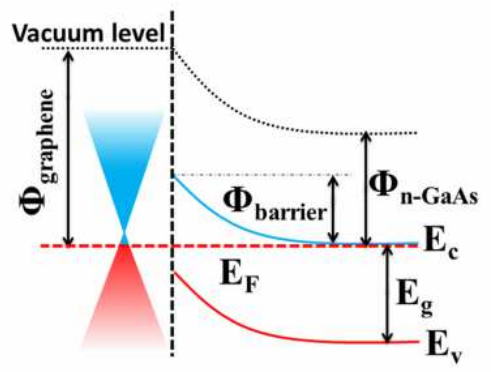

Figure 4 Band structure of graphene/GaAs Schottky junction and the effect of graphene layer numbers on physical parameters of graphene/GaAs solar cells. (a) Band structure of graphene/GaAs Schottky junction.

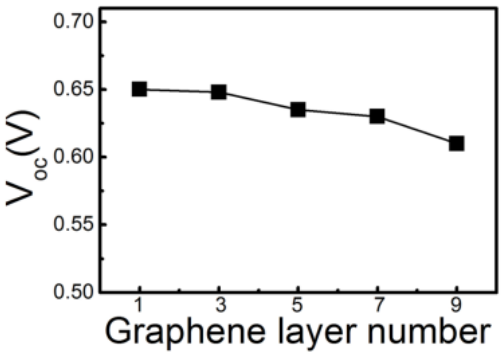

Figure 4(b) Measured Voc of the solar cells with different layers of graphene.

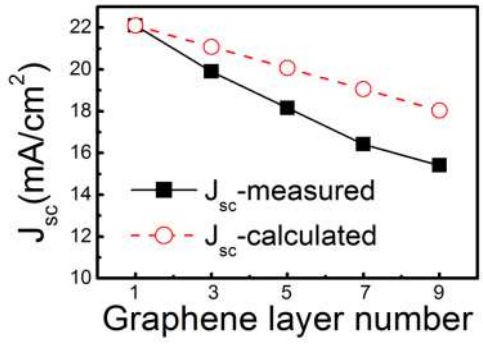

Figure 4(c) Calculated and measured Jsc with different layers of graphene.

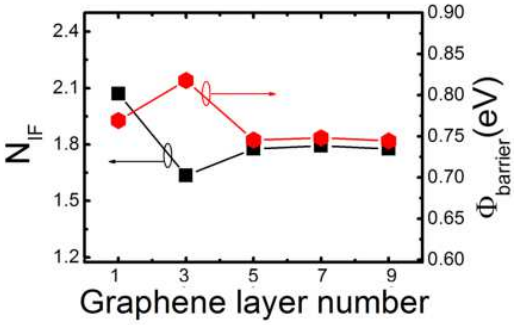

Figure 4(d) Deduced NIF and Φbarrier of the solar cells with different layers of graphene.

the experimental values of Jsc are always lower than the calculated ones. On the other hand, τbulk is keeping constant for all the samples as it is decided by the GaAs substrate, while Φbarrier and NIF vary according to layer numbers**.** Φbarrier and NIF can be obtained through measured dark current-voltage (I-V) curve fitting by equation 1 and 2, which are shown in Figure 4d. The values of NIF fall in the range of 1.7-2.1 and have no obvious relationship with graphene layer numbers. Similarly, as the graphene layer number increases, Φbarrier exhibits a fluctuating behaviour, which cannot explain the decreasing trend of Voc. Thus, it is most possibly decreasing values of τsurface causes the decreasing Voc of the devices as graphene layer number increases, which aggrees with the assumption of interlayer recombinations. It is noteworthy trilayer graphene based solar cell has the lowest NIF and highest Φbarrier.

Fuel cells

A fuel cell converts chemical energy from a fuel such as hydrogen gas into electricity via a reaction with oxygen or another oxidizing agent. Much of the attention devoted to fuel cells focuses on high power applications. When it comes to improving and before exploiting fuel cells, the principal difficulty is one of cost, and specifically the need to replace expensive noble metals such as platinum and gold as catalysts in the chemical reaction. Fuel cell electrodes must also be chemically stable over the long term, and for some applications physically flexible. Graphene and related materials are promising candidates for fuel cell electrodes, and also as membranes in proton exchange fuel cells. Where they cannot replace precious metal catalysts, the addition of two-dimensional materials may lower the amount of expensive catalyst materials required. For example, reduced graphene oxide modifies the properties of platinum electro-catalysts supported on it, leading to improved methanol oxidation when compared with commercial platinum/carbon black mixtures.

Recently, intense efforts have been made to lower the operating temperature of SOFC to minimize fabrication cost and material issues, and thus to broaden their applications[73]. However, reduction in operating temperature is followed by a significant sacrifice in electrode kinetics and ionic conductivity [74].

While sacrifice in ionic conductivity has been successfully supplemented by minimizing electrolyte thickness[73,75-77], sustaining decent electrode kinetics, especially oxygen reduction reaction (ORR) rate, at lower temperatures using conventional ceramic-based electrodes remains as a challenge. However, graphene-based electrodes such as nitrogen-doped graphene were recently found to show an excellent ORR catalytic activity comparable to that of Pt based electrodes even at room temperature.[78] In addition, graphene is reported to have exceptional thermal stability up to at least 2600 K.[79] Motivated by these superior attributes of graphene, reduced graphene oxide (rGO) variants were applied to LT-SOFC as a cathode material.

a

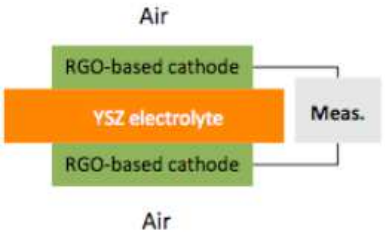

Figure:-5. (a)Simplified experimental setup for quantifying ORR activities

b

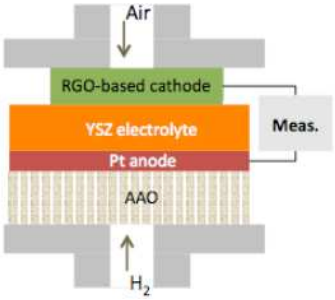

Figure:-5(b) powering performances of the RGO-based electrodes.

As shown in Figure. 5a, ORR activities of rGO based electrodes were first characterized by electrochemical impedance spectroscopy (EIS) in atmospheric air environment at various temperatures. Yttria-stabilized zirconia (YSZ) was used the electrolyte, and three different kinds of rGO variants (rGO, N-doped rGO and Pt nanoparticle incorporated rGO) were studied as electrode materials. The Faradaic resistances for ORR extracted from the resulting impedance spectra were plotted in Figure:-6 Although these rGO-based electrodes showed lower ORR activities than that of pure Pt electrodes by almost 1-2 orders of magnitude under a given temperature, the gap became negligible as the operation time elapses (data not shown). Although Pt have been unrivaled as a cathode material for low temperature catalysts, metal electrodes tend to degrade over time due to Ostwald ripening,which again results in significant cell performance degradations. In the presentation, the full cell performances using these rGO based electrodes will be presented as well (Figure 5b).

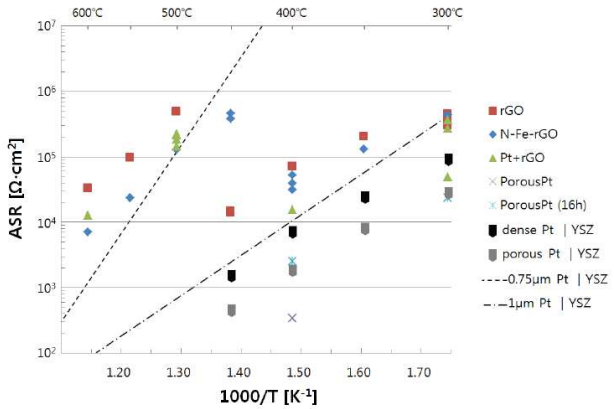

Figure: - 6 Arrhenius plot comparing ORR activities of rGO variants and Pt electrodes.

It is also noted that all the rGO variants studied here suffered from an abrupt increase in the resulting Faradaic resistance at a temperature

of >~400°C. It is attributed to the oxidation of rGO materials, and resulting change in its volume and the contact with the YSZ electrolyte. Although rGO variants may not be a stable material for operating > ~350°C, an ultra-thin electrolyte based cell can be a viable solution to implement an LTSOFC operating at a very low temperature (~300°C).

Supercapacitors

Electrochemical capacitors store energy in an electric field set up between conducting plates separated by an insulating material. Supercapacitors, which divide into electrostatic double-layer capacitors, hybrid and pseudocapacitors, are ideal for high power applications in which the required energy density is an order of magnitude greater than is possible with lithium-ion ba4eries. Such applications include electric and hybrid motor vehicles, heavy lifting, load levelling and backup power for electric utilities and industrial plant. Supercapacitors are necessarily large devices, and the materials of which they are made are produced in bulk into electrodes 100 to 200 microns thick. Most double-layer capacitors have carbon electrodes impregnated with organic electrolytes. Another type of supercapacitor is based on lithium-ion hybrid cells, in which a graphite lithium-ion anode is coupled with an activated carbon cathode. In this case the energy density is around twice that of double-layer capacitors.

The performance of supercapacitors is dependent on the electrode surface area accessible to the electrolyte, and this is where 2D crystals such as graphene have the advantage over graphite and activated carbon. In practice this can include graphene-based platelets with spacer materials such as carbon nanotubes, mesoporous carbon spheres, water and ionic liquids, and resins chemically activated to create a porous structure. large material surface areas do not always translate into high-performance supercapacitors, especially if the material packing density is low. It is possible to increase the packing density through evaporation drying of graphene hydrogels, and by capillary compression of reduced graphene oxide. Raising the operating voltage is another way of increasing the energy storage capacity. Double-layer capacitors are marked by their rapid charge/discharge and long cycle life, and lithium-ion batteries by a high energy storage capacity. Combine the two qualities, and the result is a lithium-ion hybrid supercapacitor, albeit with performance trade-offs common

to both types of device. Electrodes for double-layer capacitors made from microwave-expanded graphite oxide and lithium-ion battery electrodes comprising graphite, lithium and iron oxides have been studied, as have electrodes containing metal oxides based on ruthenium, manganese and molybdenum, with conducting polymers to increase the specific capacitance via chemical reduction and oxidation reactions. Graphene is included in these systems as a conductive support.

Supercapacitors are electrochemical devices that can store energy and release it with high power capability and high current density within a short time interval[80]. Thus, supercapacitors are considered to be the perfect complement for batteries or fuel cells in various applications, such as automobiles and high-performance portable electronics. The principle of energy storage in a supercapacitor is either (1) electrostatic charge accumulation on the electrode–electrolyte interface (electric double-layer capacitance) or (2) transfer of charge to the layer of redox molecules on the surface of the electrode (pseudocapacitance). In practical supercapacitors, the two storage mechanisms often work simultaneously[81]. Electrode materials intensively studied for supercapacitors include carbon,[82] metal oxides, [83] and conducting polymers, [84] with a recent focus on CNTs and graphene.

The electric double-layer capacitance is proportional to the effective specific surface area of an electrode material. Therefore, graphene, with a theoretical specific surface area of 2.63 × 10 6 m 2 /kg, together with good conductivity, controllable microstructure, and excellent thermal/mechanical stability, is promising for supercapacitor electrodes [85-88]. Using a chemically reduced graphene oxide electrode, Stoller et al [85,86]. obtained specific capacitances of 135,000 F/kg and 99,000 F/kg in aqueous and organic electrolytes, respectively. They also obtained capacitance values of 191,000 F/kg and 120,000 F/kg in organic electrolytes for reduced graphene oxides produced using simple microwave heating and propylene carbonate solution reduction, respectively. On the other hand, Wang et al [88]. reported graphene-based supercapacitors with a maximum specific capacitance of 205,000 F/kg at a power density of 10 kW/kg and an energy density of 28.5 W h/kg that also had an excellent cyclic lifetime, retaining 90% of the initial capacitance after 1200 cycles.

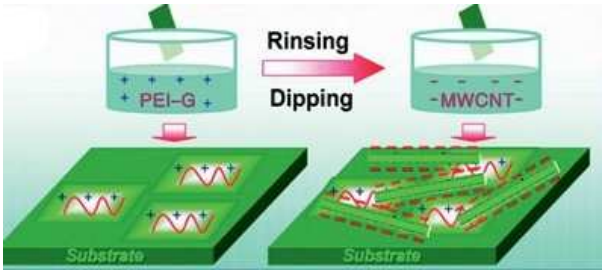

Figure:-7 Schematic illustration of the preparation of multilayered graphene–multiwalled carbon nanotube (MWCNT) hybrid electrodes for supercapacitors. PEI–G, poly(ethyleneimine)-modified graphene.

Hybrid electrodes based on two-dimensional graphene and onedimensional carbon nanotubes (CNTs) are of great interest because their structure at the nanometer to micrometer scale can be well controlled for supercapacitor applications [88-90]. For instance, a solution layer-by-layer self-assembly approach(Figure7a) was used to prepare multilayered hybrid carbon films of poly (ethyleneimine)-modified graphene sheets and acid-oxidized multiwalled CNTs to construct supercapacitors with an average specifi c capacitance of 120,000 F/kg [88]. Similarly, the inherently nanoporous three-dimensional pillared vertically aligned carbon nanotube (VA-CNT)– graphene hybrid architecture with a large surface area should allow the selection of specific thermal, mechanical, and electrical properties that are useful for many potential applications, including supercapacitors[81]. To test this possibility, Feng et al. [90] prepared a VA-CNT–graphene hybrid by the intercalated growth of VA-CNTs into thermally expanded highly ordered pyrolytic graphite. The resulting VA-CNT–graphene hybridized with a nickel hydroxide coating indeed showed a high specific capacitance with an impressive charging-rate capability

Lithium-ion batteries

Today's state-of-the-art rechargeable ba4eries are based on lithium-based cathodes and graphite anodes, and crucial to their performance is the capacity of the anode material to store lithium ions. Graphene has a larger gravimetric capacity than graphite, and the flexible nature of the material has advantages when it comes to certain applications and environments. Graphene and related materials are also appealing as fuel cell cathodes, owing to their high electrical capacity per unit weight. Graphene-based hybrid electrodes may also be employed in rechargeable ba4eries to increase electron transport, capacity, discharge current and device longevity. Where graphene is not actually incorporated into battery electrodes, it may be used as a substrate for the growth of high-performance anode/cathode nanoparticles. For example, lithium-based nanorods grown on reduced graphene oxide flakes show a significantly lower degradation over a fixed number of cycles than reduced graphene oxide or graphite.

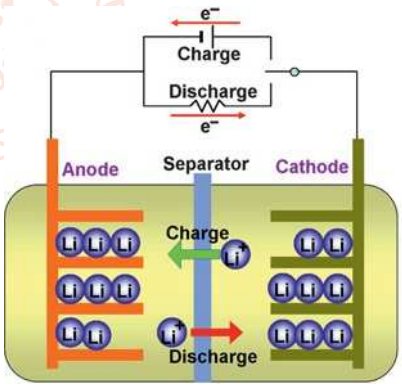

Figure:-8 the working principle of a lithium-ion battery

Lithium-ion batteries are regarded as highly attractive rechargeable batteries because of their low weight and high energy-storage capacity. Typically, a lithium-ion battery is composed of a lithium intercalation anode and cathode and an electrolyte (Figure 8**)**. The nature and microstructure of the electrode materials are crucial not only for energy and power density but also for battery safety and cycle lifetime[92,93]. Current electrode materials, including carbon black and nanofi bers, graphite, silicon, metals, and metal oxides, suffer from poor electrical conductivity and/or huge volume changes during charging/discharging[92,93].

Compared with the widely used graphite electrode, graphene has a larger specifi c surface area and twice the lithium storage capacity[94]. Moreover, recent work indicated that

the graphene two-dimensional edge plane site could aid lithium-ion adsorption and diffusion, leading to a reduced charging time and an increased power output [95]. The nanosized holes in graphene sheets were also found to be reponsible for the high-rate discharge capability of lithium-ion battery anodes [96]. Indeed, Pan et al. [95] employed graphene-sheet-based electrodes in lithiumion batterries and achieved a capacity of 540 A h/kg, which is higher than that of graphite. When carbon nanotubes and fullerenes were used as spacers to prevent individual graphene sheets from restacking, the capacity of the graphene electrodes could be further increased to 730 A h/kg and 784 A h/kg, respectively. [97] Wu et al. [98] used nitrogen- or boron-doped graphene to realize simultaneous high power and energy densities. The superior performance came from rapid surface Li + absorption, ultrafast Li + diffusion and electron transport, increased intersheet distance, and improved electrical conductivity because of the two-dimensional structure, disordered surface morphology, heteroatomic defects, and better electrode/electrolyte wettability of the doped graphene. However, it should be noted that graphene as a lithium-ion battery electrode still suffers from irreversible reactions with lithium and solid electrolyte interface formation, resulting in irreversible performance [99].

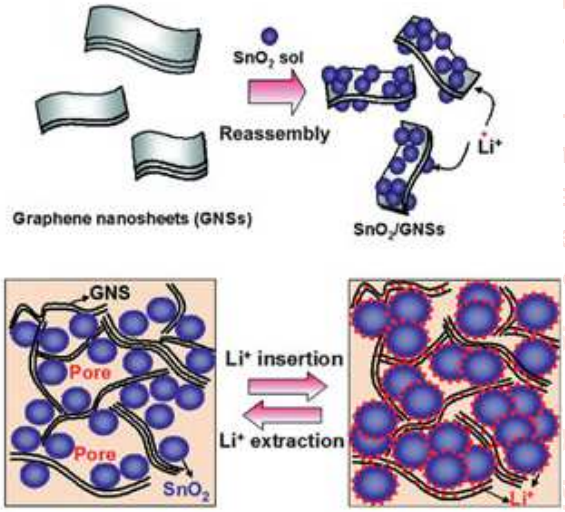

Figure:-9 (a) the structure and synthesis of a graphene–SnO 2 electrode, and (b) the improved lithium-ion storage–release cyclability of the graphene–SnO2 electrode. The nanoporous structure with SnO2 nanoparticles confi ned by graphene sheets limits the volume expansion upon lithium insertion and improves cyclic performance

Lithium-ion batteries with graphene hybrid electrodes

To address the issues discussed in the preceding subsection and to utilize the high lithium-ion reversible storage capacity of metals and metal oxides, graphene electrodes hybridized with certain metal or metal-oxide nanoparticles have been prepared to exhibit improved performance [100-103]. For example, an electrode made of nanoporous graphene sheets decorated with loosely packed SnO2 nanoparticles (Figure 9b–c) was found to exhibit a reversible capacity of 810 A h/kg with a much improved reversible cycling performance compared to those of bare graphene, SnO2 nanoparticle, and bare graphite electrodes. 83 Other metal oxides, such as Co3 O4, Fe2 O3, TiO2, and SiO2 have also been used to functionalize graphene for use as electrodes in highperformance lithium-ion batteries[101-103].

References

[1] S. Stankovich, D. A. Dikin, G. H. Dommett, K. M. Kohlhaas, E. J. Zimney, E. A. Stach, R. D. Piner, S. T. Nguyen and R. S. Ruoff, Nature, 2006, 442, 282–286.

[2] G. Eda and M. Chhowalla, Nano Lett., 2009, 9, 814–818.

[3] H. X. Chang, Z. Sun, K. Y.-F. Ho, X. Tao, F. Yan, W.-M. Kwok and Z. Zheng, Nanoscale, 2011, 3, 258–264.

[4] L. Tang, H. X. Chang, Y. Liu and J. Li, Adv. Funct. Mater, 2012, 22, 3083–3088.

[5] X. Huang, X. Qi, F. Boey and H. Zhang, Chem. Soc. Rev, 2012, 41, 666–686.

[6] H. X. Chang, L. Tang, Y. Wang, J. Jiang and J. Li, Anal. Chem, 2010, 82, 2341–2346.

[7] C. Xu, B. Xu, Y. Gu, Z. Xiong, J. Sun and X. Zhao, Energy Environ. Sci, 2013, 6, 1388–1414.

[8] T. Kuilla, S. Bhadra, D. Yao, N. H. Kim, S. Bose and J. H. Lee, Prog. Polym. Sci., 2010, 35, 1350–1375.

[9] Y. Sun, Q. Wu and G. Shi, Energy Environ. Sci, 2011, 4, 1113– 1132.

[10] L. Dai, Acc. Chem. Res, 2012, 46, 31–42.

[11] Q. Xiang, J. Yu and M. Jaroniec, Chem. Soc. Rev, 2012, 41, 782–796.

[12] C. Liu, F. Li, L. P. Ma and H. M. Cheng, Adv. Mater, 2010, 22, E28–E62.

[13] C. Huang, C. Li and G. Shi, Energy Environ. Sci, 2012, 5, 8848–8868.

[14] M. Pumera, Energy Environ. Sci, 2011, 4, 668–674.

[15] V. Georgakilas, M. Otyepka, A. B. Bourlinos, V. Chandra, N. Kim, K. C. Kemp, P. Hobza, R. Zboril and K. S. Kim, Chem. Rev, 2012, 112, 6156–6214.

[16] P. V. Kamat, J. Phys. Chem. Lett, 2011, 2, 242–251.

[17] S. Bai and X. Shen, RSC. Adv., 2012, 2, 64–98.

[18] S. Cui, S. Mao, G. Lu and J. Chen, J. Phys. Chem. Lett, 2013, 4, 2441–2454.

[19] Y. Zhu, S. Murali, W. Cai, X. Li, J. W. Suk, J. R. Potts and R. S. Ruoff, Adv. Mater., 2010, 22, 3906–3924.

[20] X. Du, I. Skachko, A. Barker and E. Y. Andrei, Nat. Nanotechnol., 2008, 3, 491–495.

[21] X. Huang, Z. Y. Yin, S. X. Wu, X. Y. Qi, Q. Y. He, Q. C. Zhang, Q. Y. Yan, F. Boey and H. Zhang, Small, 2011, 7, 1876–1902.

[22] C. Lee, X. D. Wei, J. W. Kysar and J. Hone, Science, 2008, 321, 385–388.

[23] A. A. Balandin, S. Ghosh, W. Bao, I. Calizo, D. Teweldebrhan, F. Miao and C. N. Lau, Nano Lett., 2008, 8, 902–907.

[24] R. Nair, P. Blake, A. Grigorenko, K. Novoselov, T. Booth, T. Stauber, N. Peres and A. Geim, Science, 2008, 320, 1308.

[25] Y.-M. Lin, C. Dimitrakopoulos, K. A. Jenkins, D. B. Farmer, H.-Y. Chiu, A. Grill and P. Avouris, Science, 2010, 327, 662– 662.

[26] L. Liao, Y.-C. Lin, M. Bao, R. Cheng, J. Bai, Y. Liu, Y. Qu, K. L. Wang, Y. Huang and X. Duan, Nature, 2010, 467, 305–308.

[27] F. Schwierz, Nat. Nanotechnol., 2010, 5, 487–496. 15 F. Bonaccorso, Z. Sun, T. Hasan and A. Ferrari, Nat. Photonics, 2010, 4, 611–622.

[28] H. X. Chang, Z. Sun, Q. Yuan, F. Ding, X. Tao, F. Yan and Z. Zheng, Adv. Mater., 2010, 22, 4872–4876.

[29] H. X. Chang, Z. Sun, M. Saito, Q. Yuan, H. Zhang, J. Li, Z. Wang, T. Fujita, F. Ding, Z. Zheng, F. Yan, H. Wu, M. W. Chen and Y. Ikuhara, ACS Nano, 2013, 7, 6310–6320.

[30] H. X. Chang, J. Cheng, X. Liu, J. Gao, M. Li, J. Li, X. Tao, F. Ding and Z. Zheng, Chem.–Eur. J., 2011, 17, 8896–8903.

[31] X. Wang, L. Zhi and K. M¨ullen, Nano Lett., 2008, 8, 323–327.

[32] D. Chen, L. Tang and J. Li, Chem. Soc. Rev., 2010, 39, 3157– 3180.

[33] X. Shi, H. X. Chang, S. Chen, C. Lai, A. Khademhosseini and H. K. Wu, Adv. Funct. Mater, 2012, 22, 751–759.

[34] Y. Wang, H. X. Chang, H. K. Wu and H. Liu, J. Mater. Chem. B, 2013, 1, 3521–3534.

[35] Geim, A. K. Graphene: Status and Prospects. Science324, 1530-1534 (2009).

[36] Mayorov, A. S.et al.Micrometer-Scale Ballistic Transport in Encapsulated Graphene at Room Temperature. Nano Lett.11, 2396-2399 (2011).

[37] Novoselov, K. S.et al .Room-temperature quantum hall effect in graphene. Science315, 1379-1379 (2007).

[38] Nair, R. R.et al. Fine structure constant defines visual transparency of graphene. Science320, 1308-1308 (2008).

[39] Droscher, S.et al.Quantum capacitance and density of states of graphene. Appl. Phys.Lett.96, 152104 (2010).

[40] Balandin, A. A.et al.Superior thermal conductivity ofsingle-layer graphene. Nano Lett.8, 902-907 (2008).

[41] Lee, C., Wei, X. D., Kysar, J. W. & Hone, J. Measurement of the elastic properties and intrinsic strength of monolayer graphene. Science321, 385-388 (2008).

[42] Rummeli, M. H.et al.Graphene: Piecing it Together. Adv.Mater.23, 4471-4490 (2011).

[43] Dutta, M., Sarkar, S., Ghosh, T. & Basak, D. ZnO/Graphene Quantum Dot Solid-State Solar Cell. J.Phys.Chem.C116, 20127-20131 (2012).

[44] Behura, S. K.et al.Fabrication of Bi-Layer Graphene and Theoretical Simulation for Its Possible Application in Thin Film Solar Cell. J.Nanosci.Nanotech.14, 3022-3027 (2014).

[45] Behura, S. K., Nayak, S., Mukhopadhyay, I. & Jani, O. Junction characteristics of chemically-derived graphene/p-Si heterojunction solar cell. Carbon67, 766-774 (2014).

[46] Yin, Z. Y.et al.Graphene-Based Materials for Solar Cell Applications. Adv. Energy Mater. 4, 1300574 (2014).

[47] Won, R. PHOTOVOLTAICS Graphene-silicon solar cells. Nat Photonics4, 411-411 (2010).

[48] Ye, Y.et al.High-Performance Single CdS Nanowire (Nanobelt) Schottky Junction Solar Cells with Au/Graphene Schottky Electrodes. ACSAppl.Mater.Inter.2, 3406-3410 (2010).

[49] Shi, E. Z.et al.Colloidal Antireflection Coating Improves Graphene-Silicon SolarCells. Nano Lett.13, 1776-1781 (2013).

[50] Zhang, X. Z.et al.High-efficiency graphene/Si nanoarray Schottky junction solar cells via surface modification and graphene doping. J.Mater.Chem.A1, 6593-6601 (2013).

[51] Lancellotti, L.et al.Graphene applications in Schottky barrier solar cells. Thin Solid Films522, 390-394 (2012).

[52] Feng, T. T.et al.Graphene based Schottky junction solar cells on patterned silicon-pillar-array substrate. Appl.Phys.Lett.99, 233505 (2011).

[53] Li, X. M.et al.Graphene-On-Silicon Schottky Junction Solar Cells. Adv.Mater.22, 2743-2748(2010).

[54] Miao, X. C.et al.High Efficiency Graphene Solar Cells by Chemical Doping. Nano Lett.12, 2745-2750 (2012).

[55] Belghachi, A., Helmaoui, A. & Cheknane, A. High efficiency all-GaAs solar cell. Prog.Photovoltaics18, 79-82 (2010).

[56] Ortiz, E. & Algora, C. A high-efficiency LPE GaAs solar cell at concentrations ran ingfrom 2000 to 4000 suns. Prog. Photovoltaics 11, 155-163 (2003).

[57] Yoon, J.et al.GaAs photovoltaics and optoelectronics using releasable multilayer epitaxial assemblies. Nature465, 329-380 (2010).

[58] Schnitzer, I., Yablonovitch, E., Caneau, C., Gmitter, T. J. & Scherer, A. 30-Percent External Quantum Efficiency From Surface Textured,Thin-Film Light-Emitting-Diodes. Appl.Phys.Lett.63, 2174-2176 (1993).

[59] Vorobev, V. N. & Sokolov, Y. F. Determination Of Mobility In Small Samples Of Gallium Arsenide From Magnetoresistive Effects. Sov.Phys.Semicond.5, 616 (1971).

[60] Reggiani, S.et al.Electron and hole mobility in silicon at large operating temperatures -Part I: Bulk mobility. IEEET.Electron.Dev.49, 490-499 (2002).

[61] Bucher, E. Solar-Cell Materials And Their Basic Parameters. Appl.Phys.17, 1-26 (1978).

[62] Behura, S. K., Mahala, P., Ray, A., Mukhopadhyay, I. & Jani, O. Theoretical simulation of photovoltaic response of graphene-on-semiconductors.Appl.Phys.A-Mater.111, 1159-1163 (2013).

[63] Jie, W. J., Zheng, F. G. &Hao, J. H. Graphene/gallium arsenide-based Schottky junction solar cells. Appl.Phys.Lett.103, 233111 (2013).

[64] Tereshchenko, O. E., Daineka, D. V. & Paget, D. Metallicity and disorder at the alkali-metal/GaAs(001) interface. Phys.Rev.B64, 085310 (2001).

[65] Sarkar, S., Bekyarova, E. & Haddon, R. C. Chemistry at the Dirac Point: Diels-Alder Reactivity of Graphene. Accounts Chem.Res.45, 673-682 (2012).

[66] Morozov, S. V.et al.Two-dimensional electron and hole gases at the surface of graphite. Phys.Rev.B72, 201401 (2005).

[67] Tan, S. W. & Lai, S. W. Characterization and Modeling Analysis for Metal-Semiconductor-Metal GaAs Diodes with Pd/SiO2Mixture Electrode. Plos One7, e50681 (2012).

[68] Lin, Y. X.et al.Optimization of Graphene/Silicon Heterojunction Solar Cells. 2012 38th IEEE Photovoltaic Specialists Conference (PVSC), 2566-2570 (2012).

[69] Ihm, K.et al.Number of graphene layers as a modulator of the open-circuit voltage of graphene-based solar cell. Appl.Phys.Lett.97, 032113 (2010).

[70] Aberle, A. G. Surface passivation of crystalline silicon solar cells: A review. Prog.Photovoltaics8, 473-487 (2000).

[71] Lancellotti, L.et al.Graphene applications in Schottky barrier solar cells. Thin Solid Films522, 390-394 (2012).

[72] Nair, R. R.et al.Fine structure constant defines visual transparency of graphene. Science320, 1308-1308 (2008).

[73] Huang, H., et al. High-performance ultrathin solid oxide fuel cells for low-temperature operation. Journal of the Electrochemical Society 154, B20-B24 (2007).

[74] Murray, E.P., Tsai, T. & Barnett, S.A. A directmethane fuel cell with a ceria-based anode. Nature 400, 649-651 (1999).

[75] Kang, S., Su, P.C., Park, Y.I., Saito, Y. & Prinz, F.B. Thin-film solid oxide fuel cells on porous nickel substrates with multistage nanohole array. Journal of the Electrochemical Society 153, A554-A559 (2006).

[76] Muecke, U.P., et al. Micro Solid Oxide Fuel Cells on Glass Ceramic Substrates. Advanced Functional Materials 18, 3158-3168 (2008).

[77] Su, P.C., Chao, C.C., Shim, J.H., Fasching, R. & Prinz, F.B. Solid oxide fuel cell with corrugated thin film electrolyte. Nano Letters 8, 2289-2292 (2008).

[78] Sun, Y.Q., Wu, Q.O. & Shi, G.Q. Graphene based new energy materials. Energy & Environmental Science 4, 1113-1132 (2011).

[79] Kim, K., et al. High-temperature stability of suspended single-layer graphene. Phys. Status Solidi- Rapid Res. Lett. 4, 302-304 (2010).

[80] L.L. Zhang, X.S. Zhao, Chem. Soc. Rev. 38, 2520 (2009).

[81] B.E. Conway, V. Birss, J. Wojtowicz, J. Power Sources 66, 1 (1997).

[82] E. Frackowiak, F. Beguin, Carbon 39, 937 (2001).

[83] J.P. Zheng, P.J. Cygan, T.R. Jow, J. Electrochem. Soc. 142, 2699 (1995).

[84] A. Rudge, J. Davey, I. Raistrick, S. Gottesfeld, J.P. Ferraris, J. Power Sources 47, 89 (1994).

[85] M.D. Stoller, S. Park, Y. Zhu, J. An, R.S. Ruoff, Nano Lett. 8, 3498 (2008).

[86] Y. Zhu, S. Murali, M.D. Stoller, A. Velamakanni, R.D. Piner, R.S. Ruoff, Carbon 48, 2118 (2010).

[87] Y. Zhu, M.D. Stoller, W. Cai, A. Velamakanni, R.D. Piner, D. Chen, R.S. Ruoff ,ACS Nano 4, 1227 (2010).

[88] Y. Wang, Z. Shi, Y. Huang, Y. Ma, C. Wang, M. Chen, Y. Chen, J. Phys. Chem. C 113, 13103 (2009).

[89] D. Yu, L. Dai, J. Phys. Chem. Lett. 1, 467 (2010).

[90] G.K. Dimitrakakis, E. Tylianakis, G.E. Foudakis, Nano Lett. 8, 3166 (2008).

[91] F. Du, D. Yu, L. Dai, S. Ganguli, V. Varshney, A.K. Roy, Chem. Mater. 23, 4810 (2011).

[92] M. Liang, L. Zhi, J. Mater. Chem. 19, 5871 (2009).

[93] G. Zhou, D.-W. Wang, F. Li, L. Zhang, N. Li, Z.-S. Wu, L. Wen, G.Q. Lu, H.-M. Cheng, Chem. Mater. 22, 5306 (2010).

[94] G. Wang, B. Wang, X. Wang, J. Park, S. Dou, H. Ahn, K. Kim, J. Mater. Chem. 19, 8378 (2009).

[95] D. Pan, S. Wang, B. Zhao, M. Wu, H. Zhang, Y. Wang, Z. Jiao, Chem. Mater. 21, 3136 (2009).

[96] T. Takamura, K. Endo, L. Fu, Y. Wu, K.J. Lee, T. Matsumoto, Electrochim. Acta 53, 1055 (2007).

[97] E. Yoo, J. Kim, E. Hosono, H. Zhou, T. Kudo, I. Honma, Nano Lett. 8, 2277 (2008).

[98] Z.-S. Wu, W. Ren, L. Xu, F. Li, H.-M. Cheng, ACS Nano 5, 5463 (2011).

[99] D.S. Su, R. Schlogl, ChemSusChem 3, 136 (2010).

[100] S.M. Paek, E.J. Yoo, I. Honma, Nano Lett. 9, 72 (2009).

[101] Z.S. Wu, W.C. Ren, L. Wen, L.B. Gao, J.P. Zhao, Z.P. Chen, G.M. Zhou, F. Li, H.M. Cheng, ACS Nano 4, 3187 (2010).

[102] D.H. Wang, D.W. Choi, J. Li, Z.G. Yang, Z.M. Nie, R. Kou, D.H. Hu, C.M. Wang, L.V. Saraf, J.G. Zhang, I.A. Aksay, J. Liu, ACS Nano 3, 907 (2009).

[103] S.L. Chou, J.Z. Wang, M. Choucair, H.K. Liu, J.A. Stride, S.X. Dou, Electrochem. Commun. 12, 303 (2010).